



Contents lists available at ScienceDirect

Biochimica et Biophysica Acta

journal homepage: www.elsevier.com/locate/bbamcr

Revealing the fate of cell surface human P-glycoprotein (ABCB1): The lysosomal degradation pathway



Kazuhiro Katayama^a, Khyati Kapoor^a, Shinobu Ohnuma^a, Atish Patel^a, William Swaim^b,
Indu S. Ambudkar^b, Suresh V. Ambudkar^{a,*}

^a Laboratory of Cell Biology, Center for Cancer Research, National Cancer Institute, National Institutes of Health, Bethesda, MD 20892, USA

^b Molecular Physiology and Therapeutics Branch, National Institute of Dental and Craniofacial Research, NIH, Bethesda, MD 20892, USA

ARTICLE INFO

Article history:

Received 30 April 2015

Received in revised form 2 June 2015

Accepted 4 June 2015

Available online 6 June 2015

Keywords:

P-glycoprotein

Endosome

Degradation

Half-life

Proteasome

Lysosome

ABSTRACT

P-glycoprotein (P-gp) transports a variety of chemically dissimilar amphipathic compounds including anticancer drugs. Although mechanisms of P-gp drug transport are widely studied, the pathways involving its internalization are poorly understood. The present study is aimed at elucidating the pathways involved in degradation of cell surface P-gp. The fate of P-gp at the cell surface was determined by biotinylating cell surface proteins followed by flow cytometry and Western blotting. Our data shows that the half-life of endogenously expressed P-gp is 26.7 ± 1.1 h in human colorectal cancer HCT-15 cells. Treatment of cells with Bafilomycin A1 (BafA1) a vacuolar H⁺ ATPase inhibitor increased the half-life of P-gp at the cell surface to 36.1 ± 0.5 h. Interestingly, treatment with the proteasomal inhibitors MG132, MG115 or lactacystin alone did not alter the half-life of the protein. When cells were treated with both lysosomal and proteasomal inhibitors (BafA1 and MG132), the half-life was further prolonged to 39–50 h. Functional assays done with rhodamine 123 or calcein-AM, fluorescent substrates of P-gp, indicated that the transport function of P-gp was not affected by either biotinylation or treatment with BafA1 or proteasomal inhibitors. Immunofluorescence studies done with the antibody against lysosomal marker LAMP1 and the P-gp-specific antibody UIC2 in permeabilized cells indicated that intracellular P-gp is primarily localized in the lysosomal compartment. Our results suggest that the lysosomal degradation system could be targeted to increase the sensitivity of P-gp- expressing cancer cells towards chemotherapeutic drugs.

Published by Elsevier B.V.

1. Introduction

P-glycoprotein (P-gp), also known as ABCB1, is one transporter that is frequently associated with the development of multidrug resistance (MDR) in cancer cells [1,2]. This apical 170 kDa protein is a product of the human *MDR1* or *ABCB1* gene and consists of two halves joined together by a linker region 75 amino acids in length. Each half consists of 6 membrane-spanning α helices forming the transmembrane domain (TMD) and a nucleotide-binding domain. The TMDs serve as a site for substrate binding and in turn forms the translocation pathway [3–7]. The process of active vectorial drug transport is mediated by energy derived from hydrolysis of ATP that occurs at each of the NBDs [3,8,9]. The primary physiological function of P-gp is to protect the cells from harmful toxins and xenobiotics. Cancer cells are able to exploit the protective function of this transporter and use it to their

advantage. P-gp induction contributes towards development of intrinsic (resistance even before chemotherapeutic exposure), and acquired resistance (due to frequent cycles of chemotherapeutic exposure) [1]. In accordance with this, the overexpression and thereby increase in function of P-gp have been correlated to poor prognosis due to chemotherapeutic MDR [10–18]. P-gp transports several anticancer drugs in an energy-dependent manner, thereby limiting the concentration of the anticancer agents to sub-lethal intracellular concentrations and protecting the cells [3,19–22]. Various structural and biochemical pathways have been identified since the discovery of P-gp in the 1970's [23]. Several methods have been employed to target and inhibit this MDR transporter, with very few agents showing promising results. The expression of P-gp is regulated via both synthesis and degradation of the protein. Targeting P-gp degradation has remained an attractive option; however limited data are available regarding its degradation pathway.

Cells utilize two major pathways for intracellular protein degradation: the endosomal–lysosomal system and the non-lysosomal system. Most non-lysosomal degradation occurs via the ubiquitin/26S proteasome system [24–27]. Endocytic, autophagic and phagocytic vesicles ultimately fuse with lysosomes, the terminal degradation compartment within the cell [28–31]. Cells regularly internalize extracellular material,

Abbreviations: ABC, ATP-binding cassette; P-gp, P-glycoprotein; FITC, fluorescein isothiocyanate; BafA1, bafilomycin A1; MG132, carbobenzoxy-L-leucyl-L-leucyl-L-leucinal; MG115, carbobenzoxy-L-leucyl-L-leucyl-L-norvalinal; PSI, proteasome inhibitor I; Rh123, rhodamine123; CHX, cycloheximide; lacta, lactacystin

* Corresponding author.

E-mail address: ambudkar@helix.nih.gov (S.V. Ambudkar).

plasma membrane proteins and ligands via endocytosis [29]. A coordinated balance is maintained between the removal of proteins from the cell surface and endosomal recycling pathways that return the proteins and lipids back to the plasma membrane, thus controlling the composition of the plasma membrane [32]. Here we present a detailed description of the degradation of cell surface P-gp following its internalization. (We did not study the recycling of cell surface P-gp from early endosomes or other vesicles.) Our results demonstrate that the half-life of P-gp at the cell surface of HCT-15 cells expressing high levels of endogenous P-gp without exposure to any anticancer drugs [33] is in the range of 25–27 h, which is increased to 36.1 h in cells treated with BafA1. In addition, after internalization, P-gp is localized to the lysosomes. Thus, the lysosomal pathway plays a major role in the degradation of P-gp in cancer cells, which intrinsically express this transporter at high levels without prior exposure to any anticancer drugs.

2. Experimental procedures

2.1. Reagents and chemicals

Bafilomycin A1 (BafA1) was purchased from Enzo Life Sciences (Farmingdale, NY). MG132, lactacystin, MG115, proteasome inhibitor I (PSI) and cyclosporine A (CysA) were obtained from EMD4 Biosciences (Gibbstown, NJ). Rhodamine123 (Rh123) and cycloheximide (CHX) were purchased from Sigma-Aldrich (St. Louis, MO). Drugs used in the study were dissolved in dimethyl sulfoxide (DMSO) and proteasome inhibitors were dissolved in water. Calcein-AM, Alexa Fluor® 488 Protein labeling Kit for UIC2 labeling, Alexa Fluor® 647 donkey anti-rabbit IgG (H + L) and Alexa Fluor® 647 goat anti-mouse IgG2a were purchased from Invitrogen (Grand Island, NY). E-cadherin antibody conjugated with Alexa Fluor® 647 was obtained from Santa Cruz Biotechnology (Dallas, TX). Mouse anti-BiP/GRP78 was from BD Biosciences (San Jose, CA). EEA1 rabbit mAb was procured from Cell Signaling Technology (Danvers, MA). The lysosome-associated membrane protein 1 (LAMP-1) monoclonal antibody H4A3 was obtained from the Developmental Studies Hybridoma Bank at the University of Iowa (Iowa City, IA) [34,35].

2.2. Cell lines

The human colorectal tumor HCT-15 cell line (Cat# CCL-225) was obtained from ATCC (Manassas, VA) and was used to perform the studies described here. The cells were cultured in DMEM media supplemented with 10% fetal bovine serum (FBS), 5 mM glutamine, penicillin 50 units/ml, and 50 µg/ml streptomycin, at 37 °C in 5% CO₂.

2.3. Biotinylation procedure

The water soluble EZ-link Sulfo-NHS-LC-Biotin (Thermo Scientific Pierce, Rockford, IL) was used for biotinylation of surface proteins as the sulfo-NHS (N-hydroxy-succinimide ester) cannot permeate the cell membrane, allowing only biotinylation of cell surface proteins. The cells were washed three times with cold PBS and incubated with EZ-link Sulfo-NHS-LC-Biotin (concentration range from 0.25 to 2 mg/ml) in PBS for 30 min at 4 °C. After incubation, the cells were washed three times with cold PBS and further incubated at 37 °C in 5% CO₂ for 0–48 h in DMEM supplemented with 10% FBS and other additives.

2.4. Flow cytometry

To determine the half-life of P-gp at the cell surface, biotinylated cells were trypsinized, collected and resuspended in Iscove's modified Dulbecco's medium (IMDM) supplemented with 5% FBS (IMDM/FBS).

The cells were then incubated with either P-gp isotype control IgG2a (1 µg/100,000 cells) (BD Biosciences, San Jose, CA), P-gp specific MRK16 (1 µg/100,000 cells) or UIC2 (2 µg/100,000 cells) antibodies at 37 °C for 30 min in IMDM supplemented with 5% FBS. After washing, the cells were incubated with 2 µg/100,000 cells of FITC-conjugated secondary antibody (BD Biosciences, San Jose, CA) and 1 µg/ml of PE-conjugated streptavidin (eBioscience, San Diego, CA) in IMDM/FBS medium at 37 °C for 30 min. Cells were then washed and analyzed using a FACSCalibur Flow Cytometer (Becton, Dickinson and Company, Franklin Lakes, NJ).

The drug efflux function of P-gp was measured using the fluorescent substrates Rh123 and calcein-AM, as described previously [36]. Briefly, 250,000 cells in IMDM/FBS were incubated with or without inhibitors of transport such as cyclosporine A at 5 µM along with Rh123 (1.3 µM) for 45 min or calcein-AM (0.5 µM) for 10 min at 37 °C. The cells were then washed with ice cold PBS and analyzed using the FACSCalibur flow cytometer.

2.5. Precipitation and Western blotting

Biotinylated cells were lysed with TD buffer (50 mM Tris-HCl [pH 7.4], 1% Triton X-100, 1 mM DTT, 1% aprotinin, 1 mM AEBBSF, 20 µg/ml pepstatin, 10 µg/ml leupeptin) by incubating for 30 min on ice. Four hundred µg of protein was precipitated with 40 µl of streptavidin agarose (Thermo Scientific Pierce) at 4 °C overnight with gentle rocking. After washing the agarose, biotinylated proteins were eluted by incubating with 5 mM biotin (pH 8.0) for 1.5 h at 37 °C with occasional vortexing. Biotinylated proteins were solubilized with sample buffer by incubating for 30 min at 37 °C. The proteins were then separated by SDS-PAGE and transferred onto nitrocellulose membranes. The membranes were incubated with an anti-P-gp antibody C219 1:2000 dilution followed by horseradish peroxidase-conjugated rat anti-mouse secondary antibody. The bands were visualized using the ECL (enhanced chemiluminescence) detection kit (GE Healthcare, Piscataway, NJ).

2.6. Labeling of UIC2 antibody with Alexa Fluor® 488

For single-step detection of P-gp under permeabilized and non-permeabilized conditions by confocal microscopy, UIC2 antibody was labeled with Alexa Fluor® 488 (green fluorescence) using the Alexa Fluor® 488 Protein labeling Kit as per manufacturer's protocol under laboratory conditions. This labeled UIC2 antibody is referred to as UIC2-alexa 488 in this report.

2.7. Immunofluorescence and confocal imaging of P-gp

HCT-15 (5×10^4) cells were seeded on coverslips in a 12-well plate and grown for 48 h. The cells were rinsed twice with PBS (pH 7.5) and then fixed with 2% paraformaldehyde in PBS, pH 7.5, for 30 min. Cells were then rinsed thrice with PBS (pH 7.5) and treated with 100 mM glycine in PBS for 20 min followed by washing and permeabilization with methanol at –20 °C for 5 min. (This step was skipped when cells were imaged under non-permeabilized conditions.) After washing, the cells were incubated with a blocking solution containing 5% donkey serum and 0.5% IgG free-BSA (Jackson Immuno-Research Laboratories, Inc.) in PBS for 20 min. The blocking solution was washed with PBS and the cells were incubated with UIC2-Alexa Fluor-488 antibody (4 µg/100,000 cells) or E-cadherin Alexa Fluor® 647 for 1 h at room temperature. To study colocalization of P-gp with intracellular organelles, the cells were first incubated with the respective intracellular marker antibody such as LAMP1 (lysosomal marker), EEA1 (early endosomal marker) or GRP78 (ER marker) for 1 h at room temperature and respective Alexa Fluor® 647 labeled secondary antibodies for 30 min at room temperature, followed by washing and subsequent labeling with

UIC2-alexa488 antibody. The cells were then washed and the coverslips were inverted and mounted on the slides with VECTASHIELD® (Mounting Media with DAPI) (Vector laboratories). Fluorescence images were taken at 100X using a confocal laser scanning microscope Leica TCS-SP2 attached to an upright Leica DM-RE7 microscope. All steps were performed at room temperature unless otherwise mentioned.

3. Results and discussion

Regulation of P-gp expression both at the transcriptional and post-transcriptional levels is well documented, laying out the biosynthetic pathway from P-gp synthesis starting in the endoplasmic reticulum as a core glycosylated 150 kDa protein, that then reaches the Golgi apparatus and further matures into a glycosylated 170 kDa P-gp, which is then

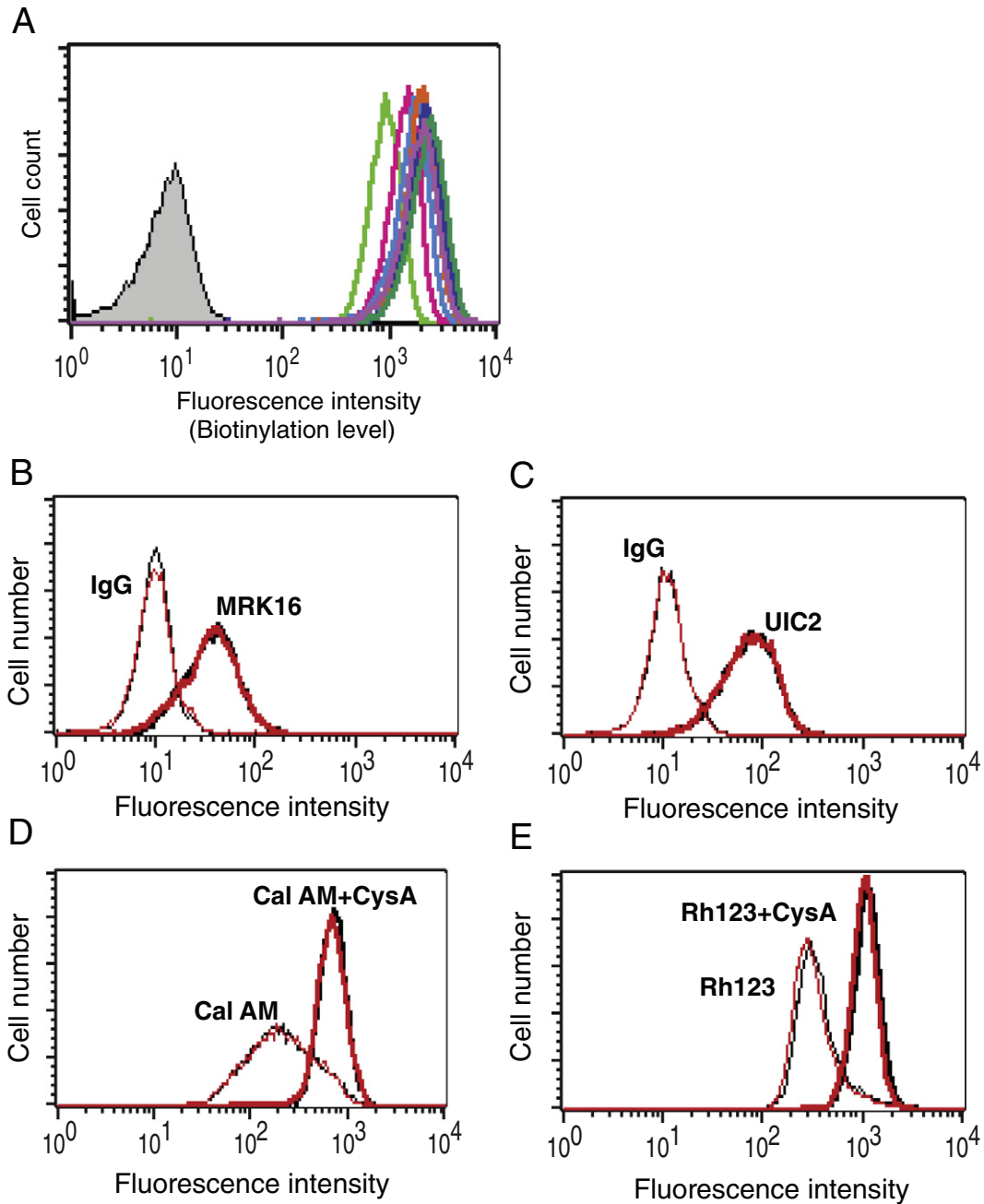


Fig. 1. Biotinylation of cell surface proteins of HCT-15 cells and its effect on detection of P-gp level and function. (A) HCT-15 cells were incubated without or with PBS containing Sulfo-NHS-LC-biotin with concentration ranging from 0.025 to 2 mg/ml for 30 min at 4 °C. The cells were then trypsinized and incubated with streptavidin-PE for 30 min on ice. These cells were then analyzed by flow cytometry and the histogram shows the level of biotin label at the cell surface. The gray filled histogram shows no biotin labeling while the colored histograms mark the level of biotinylation of cell surface proteins in the presence of various concentrations of biotin: 0.025 mg/ml (green), 0.05 mg/ml (pink), 0.1 mg/ml (blue), 0.25 mg/ml (orange), 0.5 mg/ml (dark blue), 1 mg/ml (dark green), and 2 mg/ml (purple). Biotinylation does not affect the detection of cell surface P-gp with antibodies or its function. HCT-15 cells treated without (black trace) or with biotin (red trace) were subjected to staining by P-gp-specific antibodies (B) MRK-16 or (C) UIC2 followed by FITC-conjugated anti-mouse secondary antibody, to determine the cell surface level of P-gp. The IgG2a isotype control was included in each of these experiments. The function of P-gp was compared in both biotin labeled and unlabeled cells by monitoring the transport of (D) Calcein-AM or (E) Rh123. The transport of these substrates in both biotin-labeled (red trace) and unlabeled (black trace) cells was reversed by the inhibitor CysA (5 μM; traces labeled as Cal-AM + CysA in D and Rh123 + CysA in E). The histograms from a representative experiment are shown and similar results were obtained in three additional independent experiments.

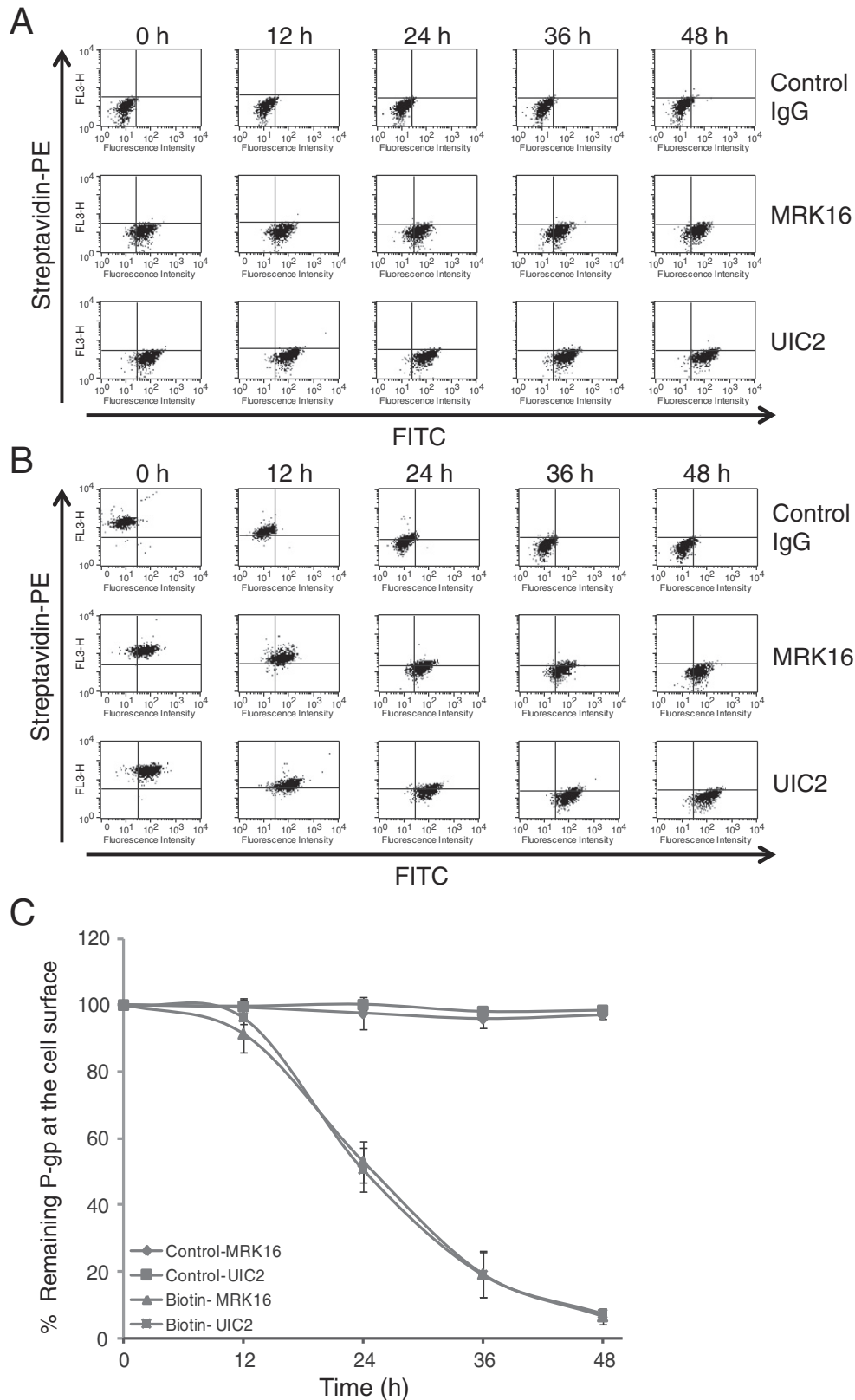


Fig. 2. The biotinylation of cell surface P-gp does not affect its detection by monoclonal antibodies. HCT-15 cells were incubated with (A) PBS or (B) Sulfo-NHS-LC-biotin for 30 min at 4 °C and then cultured at 37 °C for 0–48 h in normal growth media. The cells were trypsinized and double stained with streptavidin-PE and P-gp specific antibody MRK-16, UIC2 or IgG isotype control (followed by FITC anti-mouse secondary antibody) as described in Section 2. FACS data obtained from the FACSCalibur Flow Cytometer was subjected to quadrant analysis in FlowJo (Ashland, OR). Having the FITC (FL1) and streptavidin-PE (FL3) channels set on the X-axis and Y-axis respectively, the upper and lower right areas showed biotinylated and unbiotinylated P-gp, respectively. The percentages of cells included in the upper right area of histogram were calculated to determine biotinylated P-gp at the indicated time points in the figures. The percentages of biotinylated P-gp remaining were obtained by dividing the values at each time point by that at 0 h. (C) The total P-gp level was compared to that of remaining biotinylated P-gp at the cell surface at indicated times detected with both MRK-16 and UIC2 antibodies. The data points are plotted as the mean \pm SD from three independent experiments.

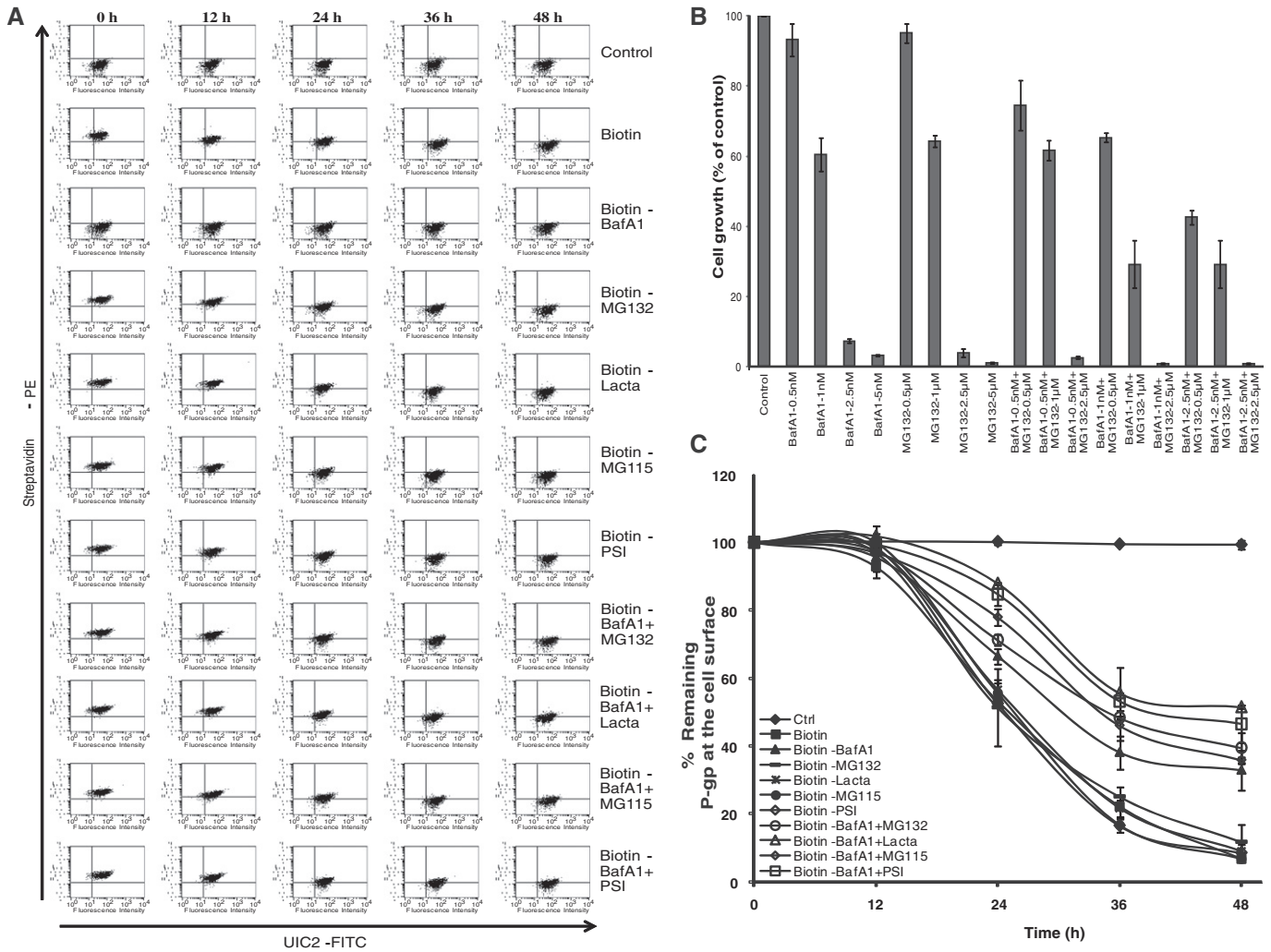


Fig. 3. Effect of various lysosomal or proteasomal inhibitors on the half-life of cell surface P-gp. (A) HCT-15 cells were incubated in the presence of indicated concentrations of lysosomal inhibitor (BafA1), proteasomal inhibitor (MG132) or a combination of both for 48 h. Cell growth was determined by MTT assays and the values represent mean \pm SD from three independent experiments. HCT-15 cells were incubated without or with biotin for 30 min at 4 °C. These were further cultured for 0–48 h in the absence or presence of (B) the lysosomal inhibitor (BafA1), proteasomal inhibitors (MG132, lactacystin, MG115 or PSI) or a combination of both as indicated. The cell surface level of biotinylated P-gp was followed using streptavidin-PE and P-gp-specific UIC2 antibody staining for 0–48 h. (C) The level of cell surface P-gp under each of these conditions was plotted as mean \pm SD from three independent experiments. The half-life of cell surface P-gp determined under various drug treatments including 1 mM ammonium chloride is summarized in Table 1.

ready for trafficking and function as an efflux pump at the cell surface [37,38]. Recently it was reported that phosphorylation of the transporter by Pim-1 kinase among other post-translational modifications is key towards protecting it from proteolytic and proteasomal degradation, thereby stabilizing the transporter and allowing it to be glycosylated and delivered to the cell membrane [39]. However, limited information is available regarding the fate of cell surface P-gp. Here we sought to identify the pathway governing the degradative fate of P-gp following its internalization in HCT-15 cells. These colon cancer cells express high levels of endogenous P-gp (without exposure to any anti-cancer drugs). In this study, we did not use cells subjected to any stress including drug-selection or disease condition.

3.1. Determination of the half-life of P-gp at the cell surface

To evaluate the degradation mechanism of P-gp, we first determined its half-life at the cell surface of HCT-15 cells that endogenously express P-gp. HCT-15 cells were first labeled with biotin and then cultured in media as described in Section 2. Biotin and streptavidin bind with one of the strongest non-covalent bonds known, making the complex resistant to proteolysis and extremes of heat and pH [40,41]. FACS

Table 1

Half-life of biotinylated P-gp at the cell surface under various treatments of HCT-15 cells with lysosomal and proteasomal inhibitors.

Treatment(s)	Half-life (h)
Biotin	26.7 \pm 1.1
Biotin-BafA1	36.1 \pm 0.5
Ammonium Chloride	34.9 \pm 1.2
Biotin-MG132	26.0 \pm 1.2
Biotin-Lacta	26.0 \pm 1.5
Biotin-MG115	26.0 \pm 1.2
Biotin-PSI	26.0 \pm 1.1
Biotin-BafA1 + MG132	39.0 \pm 1.0
Biotin-BafA1 + Lacta	50.0 \pm 2.9
Biotin-BafA1 + MG115	38.0 \pm 1.9
Biotin-BafA1 + PSI	45.0 \pm 2.7

HCT-15 cells were treated with Sulfo-NHS-LC-biotin (1 mg/ml) for 30 min at 4 °C and then grown in DMEM for 0 to 48 h at 37 °C in the presence or absence of BafA1 (1 nM), Ammonium Chloride (1 mM), MG132 (1 μM), lacta (5 μM) and PSI (100 nM) alone or together. The level of biotinylated P-gp remaining at the cell surface was determined as given in the legend to Figs. 2 and 3. The values represent the mean \pm SD from three independent experiments. BafA1, bafilomycin A1; Lacta, lactacystin; PSI, proteasome inhibitor I.

measurements serve as the most useful tools for the measurement of surface biotinylation and thereby detection of P-gp at the cell surface. We initiated our examination by determining the concentration of biotin that could biotinylate all cell surface proteins and further validated the reactivity of P-gp specific MRK16 or UIC2 antibodies and the function of P-gp with Rh123 or calcein-AM accumulation assays under biotinylation conditions. This would confirm if biotinylation of the cell membrane would affect the expression or reactivity of P-gp-specific antibodies or the function of P-gp.

As shown in Fig. 1A, 1 mg/ml of EZ-linked sulfo-NHS-LC-biotin allowed the highest levels of biotinylation when testing a range of concentrations between 0.025 and 2 mg/ml. Under these conditions, reactivity of either MRK16 or UIC2 with cell surface P-gp was unchanged in biotinylated cells compared with control cells (Fig. 1B and C). Biotinylation did not affect P-gp function as an efflux pump in either calcein-AM or Rh123 accumulation assays because intracellular calcein-AM or Rh123 levels in biotinylated cells were the same as those in control cells and the inhibition of efflux function by 5 μ M

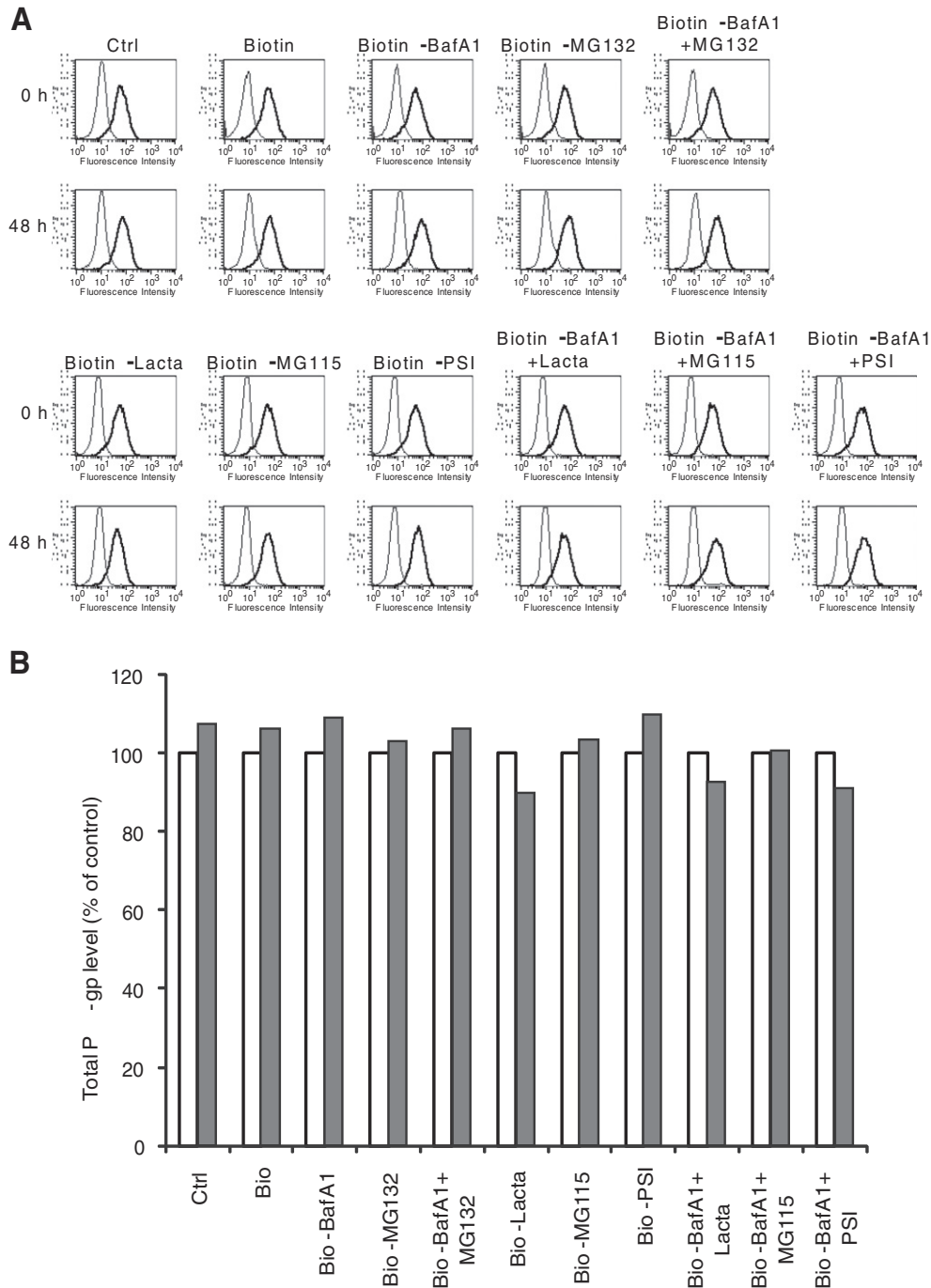


Fig. 4. The level of total cell surface P-gp is not affected by treatment with lysosomal or proteasomal inhibitors. (A) HCT-15 cells were treated without (control) or with biotin and then incubated with the indicated drugs for 0–48 h. The cells were trypsinized and incubated with isotype control IgG or P-gp specific antibody followed by FITC-labeled anti-mouse secondary antibody and then subjected to analysis by flow cytometry. (B) The median fluorescence in each case was measured. Open bars (0 h) and filled bars (48 h) show the relative cell surface P-gp expression under various drug treatments calculated as a percentage of control (untreated). The histograms in A are from a representative experiment and the values in B are average from two independent experiments.

cyclosporine A (CysA) was also not affected by biotinylation of cells (Fig. 1D and E).

We then checked the half-life of P-gp at the cell surface by measuring the clearance of biotinylated P-gp from the cell surface under normal culture conditions. In control cells, total P-gp expression levels remained constant between 0 and 48 h, as validated using two human P-gp-specific monoclonal antibodies MRK16 and UIC2 (Fig. 2A and C). Comparatively, biotinylated P-gp levels diminished in a time-dependent manner after biotinylation (Fig. 2B and C). The half-lives of biotinylated P-gp at the cell surface were determined as 26.6 ± 1.8 h in MRK16-antibody reaction experiments and 26.7 ± 1.1 h in UIC2-antibody reaction experiments (Fig. 2C). These results demonstrate that the half-life of P-gp at the cell surface is about 25 to 27 h with no difference in detection of biotinylated P-gp using either the MRK16 or UIC2 antibodies.

3.2. Treatment with lysosomal inhibitor bafilomycin A1 prolongs the life of cell surface P-gp

In this study, we characterized the degradation pathway for cell surface P-gp. BafA1, a macrolide antibiotic, inhibits vesicular fusion with the lysosome, the last step in the lysosomal degradation pathway. BafA1 is a highly potent and selective vacuolar type H^+ -ATPase (V-ATPase) inhibitor that inhibits the acidification of lysosomes, thus blocking the protein degradation activity [42,43]. In addition, MG132, a peptide aldehyde (carbobenzoxy-leu-leu-leucinal), is a potent cell permeable inhibitor of the proteasomal degradation pathway, preventing the degradation of ubiquitinated proteins, showing no effect on cellular ATPases [44]. These two inhibitors of the critical checkpoints in protein degradation pathways serve as important tools to identify the degradative fate of P-gp. Hence, we examined the effect of BafA1 and/or MG132 on the removal of biotinylated P-gp from the cell surface (Fig. 3A). We also evaluated the effect of BafA1 and MG132 on cell death by MTT assays. BafA1 at 1 nM and MG132 at 1 μ M resulted in >60% cell survival over a treatment period spanning 48 h (Fig. 3B), hence we selected the concentrations of 1 nM for BafA1 and 1 μ M for MG132 for use in subsequent studies. A 48 h treatment of biotinylated HCT-15 cells yielded approximately 40% P-gp expression on the cell surface compared to untreated cells, with only 10% biotinylated P-gp expression obtained in cells treated without BafA1 (Fig. 3A, B and C). The half-life of P-gp in BafA-treated biotinylated cells was 36.1 ± 0.5 h, whereas the half-life in cells treated with MG132 was 26.2 ± 2.3 h, which was almost the same as that in control cells.

We also tested ammonium chloride, another inhibitor that blocks acidification of lysosomes [45], on the rate of internalization of cell surface P-gp. The half-life of biotinylated P-gp could be determined as 26 h in control cells. Ammonium chloride (1 mM) treatment prolonged it to 34.9 h, attaining similar numbers as BafA1 (Table 1). These results suggest the fate of internalized P-gp is to end up in the acidic compartments (most likely lysosomal) for degradation, since BafA1 or ammonium chloride prolonged the cell surface retention of P-gp.

3.3. The combination of lysosomal inhibitor and proteasomal inhibitors further prolongs the half-life of P-gp

It is clear from the data in Fig. 3 that treatment with MG132, which inhibits the 26S proteasomal pathway, has no effect on the half-life of P-gp. We also checked the effect of other proteasomal inhibitors such as lactacystin, MG115 and PSI on the internalization of cell surface P-gp. A cell survival MTT assay revealed that 5 μ M lactacystin, 0.5 μ M MG115 and 100 nM PSI in the presence of 1 nM BafA1 allowed over 60% cell growth under these conditions (data not shown). However, interestingly cells that were treated with a combination of BafA1 (1 nM) and MG132 (1 μ M) showed an increase in the half-life of cell surface biotinylated P-gp from 36.1 ± 0.5 h to 39 ± 0.1 h (Fig. 3C). Thus, a combination of lysosomal and

proteasomal inhibitors significantly increased the cell surface retention of P-gp (Fig. 3A, C and Table 1).

Similar to MG132, other proteasome inhibitors also together with BafA1 prolonged the half-life of biotinylated P-gp and the values were 50 ± 2.9 h in the presence of lactacystin (5 μ M), 38 ± 1.9 h, for MG115 (1 μ M) and 45 ± 2.7 h with PSI (100 nM) together with 1 nM BafA1 (Table 1). In contrast, lactacystin, MG115 or PSI alone did not affect the rate of removal of P-gp from the cell surface compared with no drug treatment. Total P-gp levels after 48 h culture were virtually unchanged in all of the samples (Fig. 4A and B). The treatment with BafA1 (lysosomal inhibitor) or MG132 (proteasomal inhibitor) did not

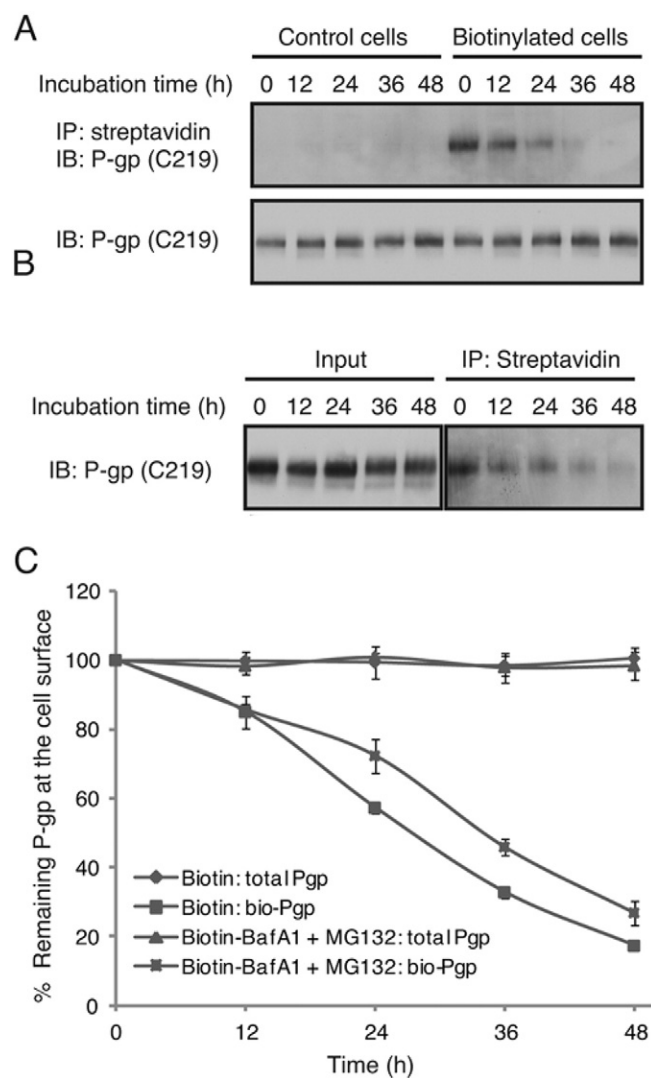


Fig. 5. Decrease in level of cell surface biotinylated P-gp was analyzed by precipitation with streptavidin. (A) HCT-15 cells were incubated with PBS (control cells) or Sulfo-NHS-LC-biotin for 30 min at 4 °C and then cultured for 0–48 h in normal growth conditions. The cells were trypsinized at indicated times and proteins were precipitated from the lysate of 1 million cells for each condition using streptavidin agarose as described in Section 2. P-gp was detected by Western blotting using the P-gp-specific antibody C219. The total P-gp level in the lysates remained constant over 0–48 h, as detected by C219 antibody without precipitation with streptavidin (the blot in lower panel). (B) The cells were grown in the presence of 1 nM BafA1 + 1 μ M MG132 and then the biotinylated P-gp was precipitated using streptavidin agarose. The level of biotinylated P-gp (right panel) was compared to the total P-gp in the cell lysates at various time intervals (left panel). The blots from a representative experiment are shown. Similar results were obtained in two additional experiments. (C) The level of total and biotinylated cell-surface P-gp was plotted at indicated times ranging from 0 to 48 h as mean \pm SD from three independent experiments. The experimental conditions are given in the figure. IB, immunoblot and IP, precipitation with streptavidin-agarose beads.

affect the function of P-gp (data not shown). These data suggest that there still exists an unexplored mechanism by which the proteins that end up in the lysosome and are not degraded are then directed to the proteasome for degradation.

3.4. Measuring the level of biotinylated P-gp by precipitating with streptavidin followed by Western blotting with P-gp-specific antibody

Precipitation with streptavidin followed by Western blot analysis was carried out on biotinylated HCT-15 cells. The biotinylated cell lysates were incubated with streptavidin agarose, and the precipitated P-gp was then detected by Western blot using an anti-P-gp antibody C219 (Fig. 5A). The expression of biotinylated P-gp decreased over a period of 48 h in a time-dependent manner after biotinylation under normal culture conditions, although total P-gp levels were constant up to 48 h in control and biotinylated cells. A comparison of the expression levels at each time point with those at 0 h revealed that the half-life of biotinylated P-gp was 27.6 ± 1.8 h and that this number was consistent with the numbers obtained from FACS experiments (Fig. 2C). A similar experiment was performed with BafA1-treated cells, as shown in Fig. 5B, biotinylated P-gp could be clearly detected until 48 h in cells treated with BafA1, although it could not be detected at 48 h in cells without treatment with BafA1. The half-life of biotinylated P-gp in BafA1-treated cells was 35.7 ± 0.7 h. These results were consistent with the numbers obtained from FACS experiments (Fig. 2C).

3.5. Conjugation of Alexa Fluor® 488 label with UIC2 antibody does not affect detection of P-gp at the cell surface

The UIC2 antibody was conjugated with Alexa Fluor® 488 for single-step detection of cell surface P-gp in non-permeabilized and for detection of intracellular P-gp in permeabilized HCT-15 cells. Fig. 6A shows the membrane localization of P-gp in non-permeabilized cells using UIC2-alexa488 antibody (green fluorescence). To ensure that the cell membrane was not completely destroyed upon permeabilization, the non-permeabilized HCT-15 cells were stained with E-cadherin Alexa Fluor® 647 (red) (Fig. 6B). Fig. 6C shows the labeling of E-cadherin in permeabilized plasma membrane. The nuclei were stained blue with DAPI present in the VECTASHIELD® in all samples.

3.6. P-gp co-localizes with LAMP1 lysosomal marker in permeabilized cells

Intracellular localization of P-gp was checked by double staining of HCT-15 cells with lysosomal marker (LAMP1) antibody and P-gp specific UIC2-Alexa Fluor-488 antibody. The cells were permeabilized with methanol and stained with LAMP1 antibody followed by Alexa Fluor® 647-labeled secondary antibody (red). These cells were then stained with UIC2-alexa 488 antibody (green). Fig. 6D shows the double staining of HCT-15 cells. The left panel shows P-gp labeling (green), the middle shows lysosomal staining (red) and the right panel shows a merge of these two. The yellow color in the merged image represents co-localization of P-gp (green) and LAMP1 (red) staining. Under these conditions, P-gp was not detected in either early endosomes or in the

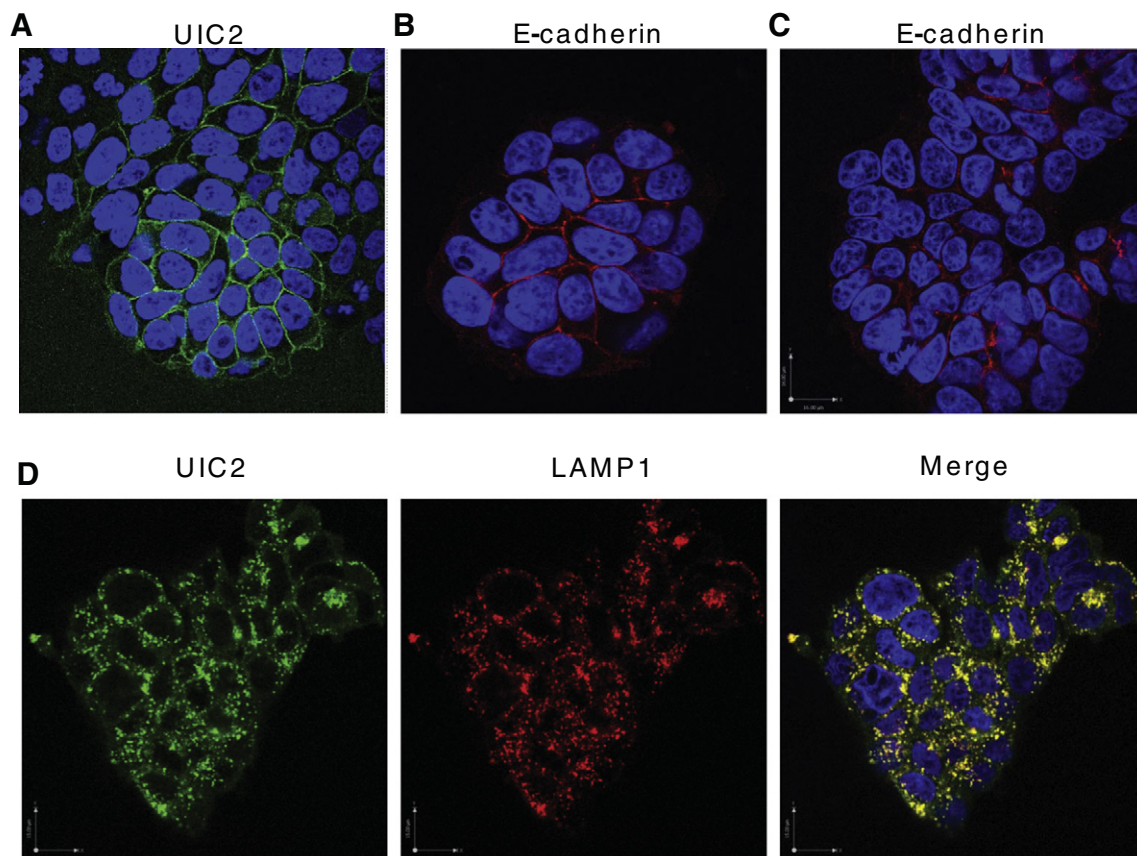


Fig. 6. Localization of biotinylated P-gp in permeabilized and non-permeabilized HCT-15 cells. (A) Detection of cell surface P-gp using UIC2-alexa488 antibody (green) in non-permeabilized HCT-15 cells. (B) Staining of cell membrane using cell surface marker E-cadherin-alexa647 antibody (red) in non-permeabilized cells. (C) Staining of cell membrane using E-cadherin-alexa647 antibody in permeabilized cells as described in Section 2. (D) The cells were permeabilized and double stained with P-gp specific antibody UIC2-alexa488 (green) and lysosomal marker LAMP1-alexa647 (red). The third panel shows an overlay of both stains with these two antibodies. Yellow color indicates staining with both antibodies. The nuclei were stained with DAPI present in VECTASHIELD® in all samples.

ER as its co-localization with EEA1 (early endosome marker) and BiP/GRP78 (ER marker) in permeabilized cells was not observed (data not shown).

This is the first report to determine the cellular fate of cell surface P-gp at steady state. The half-life of P-gp at the plasma membrane is quite long (25–27 h) compared to that of other proteins. After internalization, the P-gp protein is degraded in lysosomes. However, if the lysosomal degradation pathway is blocked, then the transporter is degraded by the proteasomal pathway, as the half-life of P-gp is significantly extended in cells treated with both lysosomal and proteasomal inhibitors (Table 1). These findings summarized in Fig. 7 schematic (see legend to this figure for details) suggest that it should be possible to screen small molecule and natural compound libraries to identify compounds that would significantly accelerate the internalization followed by degradation of cell surface P-gp, providing a way to sensitize cancer cells to anticancer drugs and improve the chemotherapeutic outcome. Recently Peng et al. identified compounds that could interact in two different modalities with ABCG2 (another anticancer drug efflux ABC transporter linked to the development of MDR), by inhibiting its efflux function and also accelerating its lysosomal degradation upon treatment, thereby reducing MDR in cancer cells [46]. It should also be possible to design therapeutics and to screen small molecule libraries that would have a similar effect on P-gp, drugs that would accelerate the degradation of this resilient transporter that renders cells impervious to chemotherapeutic agents.

Contributions

Authorship: K. Katayama and SVA designed experiments, K. Katayama, KK, SO performed experiments and analyzed data. K.

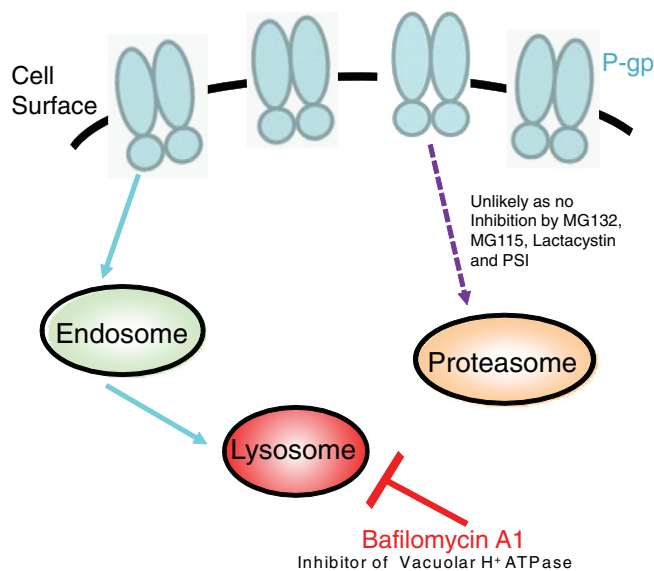


Fig. 7. Schematic showing the proposed model for degradation of cell surface P-gp. The half-life of cell surface P-gp (depicted in cyan color) is significantly long (25–27 h). The recycling of cell surface P-gp from early endosomes or other vesicles was not studied. Treatment with BafA1 or ammonium chloride blocks acidification of lysosomal or other acidic organelles and extends the half-life of P-gp at the cell surface. The treatment with only proteasomal inhibitors including MG132, MG115, lactacystin or PSI has no effect on P-gp half-life at the cell surface suggesting that the proteasomal pathway may not be involved in degradation of cell surface P-gp. However, a combination treatment with proteasomal inhibitor MG132 along with the lysosomal inhibitor BafA1 resulted in prolonged P-gp retention time (increased half-life) at the cell surface, indicating that the proteasomal pathway becomes operative when the lysosomal pathway is blocked. The localization of P-gp to lysosomes, but not to early endosomes at steady-state indicates that the lysosomal pathway plays a major role in the degradation of P-gp (BafA1 or ammonium chloride also inhibit endosomal acidification).

Katayama, KK, AP and SVA wrote the manuscript, WS, and IA helped with the confocal microscopy.

Conflict of interest

The authors disclose no potential conflicts of interest.

Acknowledgments

We thank Dr. Hwei Ling Ong for the help with confocal microscopy experiments and George Leiman for the editorial assistance. This work was supported by the Intramural Research Program of the NIH, National Cancer Institute, Center for Cancer Research and National Institute of Dental and Craniofacial Research.

References

- [1] M.M. Gottesman, T. Fojo, S.E. Bates, Multidrug resistance in cancer: role of ATP-dependent transporters, *Nat. Rev. Cancer* 2 (2002) 48–58.
- [2] M.M. Gottesman, Mechanisms of cancer drug resistance, *Annu. Rev. Med.* 53 (2002) 615–627.
- [3] S.V. Ambudkar, I.W. Kim, Z.E. Sauna, The power of the pump: mechanisms of action of P-glycoprotein (ABCB1), *Eur. J. Pharm. Sci.* 27 (2006) 392–400.
- [4] S.G. Aller, J. Yu, A. Ward, Y. Weng, S. Chittaboina, R. Zhuo, P.M. Harrell, Y.T. Trinh, Q. Zhang, I.L. Urbatsch, G. Chang, Structure of P-glycoprotein reveals a molecular basis for poly-specific drug binding, *Science* 323 (2009) 1718–1722.
- [5] S. Dey, M. Ramachandra, I. Pastan, M.M. Gottesman, S.V. Ambudkar, Evidence for two nonidentical drug-interaction sites in the human P-glycoprotein, *Proc. Natl. Acad. Sci. U. S. A.* 94 (1997) 10594–10599.
- [6] T.W. Loo, M.C. Bartlett, D.M. Clarke, Simultaneous binding of two different drugs in the binding pocket of the human multidrug resistance P-glycoprotein, *J. Biol. Chem.* 278 (2003) 39706–39710.
- [7] M.R. Lugo, F.J. Sharom, Interaction of LDS-751 and rhodamine 123 with P-glycoprotein: evidence for simultaneous binding of both drugs, *Biochemistry* 44 (2005) 14020–14029.
- [8] A.E. Senior, Two ATPases, *J. Biol. Chem.* 287 (2012) 30049–30062.
- [9] S.V. Ambudkar, S. Dey, C.A. Hrycyna, M. Ramachandra, I. Pastan, M.M. Gottesman, Biochemical, cellular, and pharmacological aspects of the multidrug transporter, *Annu. Rev. Pharmacol. Toxicol.* 39 (1999) 361–398.
- [10] D. Steinbach, O. Legrand, ABC transporters and drug resistance in leukemia: was P-gp nothing but the first head of the Hydra? *Leukemia* 21 (2007) 1172–1176.
- [11] M. Pallis, R. Hills, P. White, M. Grundy, N. Russell, A. Burnett, Analysis of the interaction of induction regimens with p-glycoprotein expression in patients with acute myeloid leukaemia: results from the MRC AML15 trial, *Blood Cancer J.* 1 (2011) e23.
- [12] Y. Kuwazuru, A. Yoshimura, S. Hanada, A. Utsunomiya, T. Makino, K. Ishibashi, M. Kodama, M. Iwahashi, T. Arima, S. Akiyama, Expression of the multidrug transporter, P-glycoprotein, in acute leukemia cells and correlation to clinical drug resistance, *Cancer* 66 (1990) 868–873.
- [13] J.P. Marie, R. Zittoun, B.I. Sikic, Multidrug resistance (mdr1) gene expression in adult acute leukemias: correlations with treatment outcome and in vitro drug sensitivity, *Blood* 78 (1991) 586–592.
- [14] R. Pirker, J. Wallner, K. Geissler, W. Linkesch, O.A. Haas, P. Bettelheim, M. Hopfner, S. Scherrer, P. Valent, L. Havelec, et al., MDR1 gene expression and treatment outcome in acute myeloid leukemia, *J. Natl. Cancer Inst.* 83 (1991) 708–712.
- [15] L. Campos, D. Guyotat, E. Archimbaud, P. Calmard-Oriol, T. Tsuruo, J. Troncy, D. Treille, D. Fiere, Clinical significance of multidrug resistance P-glycoprotein expression on acute nonlymphoblastic leukemia cells at diagnosis, *Blood* 79 (1992) 473–476.
- [16] D.C. Zhou, J.P. Marie, A.M. Suberville, R. Zittoun, Relevance of mdr1 gene expression in acute myeloid leukemia and comparison of different diagnostic methods, *Leukemia* 6 (1992) 879–885.
- [17] P. Wood, R. Burgess, A. MacGregor, J.A. Yin, P-glycoprotein expression on acute myeloid leukaemia blast cells at diagnosis predicts response to chemotherapy and survival, *Br. J. Haematol.* 87 (1994) 509–514.
- [18] S. Zochbauer, A. Gsur, R. Brunner, P.A. Kyrle, K. Lechner, R. Pirker, P-glycoprotein expression as unfavorable prognostic factor in acute myeloid leukemia, *Leukemia* 8 (1994) 974–977.
- [19] G. Szakacs, J.K. Paterson, J.A. Ludwig, C. Booth-Genthe, M.M. Gottesman, Targeting multidrug resistance in cancer, *Nat. Rev. Drug Discov.* 5 (2006) 219–234.
- [20] X. Li-Blatter, A. Seelig, Exploring the P-glycoprotein binding cavity with polyoxyethylene alkyl ethers, *Biophys. J.* 99 (2010) 3589–3598.
- [21] D.A. Gutmann, A. Ward, I.L. Urbatsch, G. Chang, H.W. van Veen, Understanding polyspecificity of multidrug ABC transporters: closing in on the gaps in ABCB1, *Trends Biochem. Sci.* 35 (2010) 36–42.
- [22] F.J. Sharom, The P-glycoprotein multidrug transporter, *Essays Biochem.* 50 (2011) 161–178.
- [23] J.A. Endicott, V. Ling, The biochemistry of P-glycoprotein-mediated multidrug resistance, *Annu. Rev. Biochem.* 58 (1989) 137–171.
- [24] N. Mizushima, D.J. Klionsky, Protein turnover via autophagy: implications for metabolism, *Annu. Rev. Nutr.* 27 (2007) 19–40.

- [25] S. Kornfeld, I. Mellman, The biogenesis of lysosomes, *Annu. Rev. Cell Biol.* 5 (1989) 483–525.
- [26] N.A. Bright, M.J. Gratian, J.P. Luzio, Endocytic delivery to lysosomes mediated by concurrent fusion and kissing events in living cells, *Curr. Biol.* 15 (2005) 360–365.
- [27] J. Smalle, R.D. Vierstra, The ubiquitin 26S proteasome proteolytic pathway, *Annu. Rev. Plant Biol.* 55 (2004) 555–590.
- [28] A. Vellodi, Lysosomal storage disorders, *Br. J. Haematol.* 128 (2005) 413–431.
- [29] C. de Duve, Lysosomes revisited, *Eur. J. Biochem.* 137 (1983) 391–397.
- [30] W. Hunziker, H.J. Geuze, Intracellular trafficking of lysosomal membrane proteins, *Bioessays* 18 (1996) 379–389.
- [31] P.R. Pryor, J.P. Luzio, Delivery of endocytosed membrane proteins to the lysosome, *Biochim. Biophys. Acta* 1793 (2009) 615–624.
- [32] F.R. Maxfield, T.E. McGraw, Endocytic recycling, *Nat. Rev. Mol. Cell Biol.* 5 (2004) 121–132.
- [33] J.W. Critchfield, C.J. Welsh, J.M. Phang, G.C. Yeh, Modulation of adriamycin accumulation and efflux by flavonoids in HCT-15 colon cells. Activation of P-glycoprotein as a putative mechanism, *Biochem. Pharmacol.* 48 (1994) 1437–1445.
- [34] J.W. Chen, T.L. Murphy, M.C. Willingham, I. Pastan, J.T. August, Identification of two lysosomal membrane glycoproteins, *J. Cell Biol.* 101 (1985) 85–95.
- [35] J.W. Chen, G.L. Chen, M.P. D'Souza, T.L. Murphy, J.T. August, Lysosomal membrane glycoproteins: properties of LAMP-1 and LAMP-2, *Biochem. Soc. Symp.* 51 (1986) 97–112.
- [36] S. Shukla, C. Schwartz, K. Kapoor, A. Kouanda, S.V. Ambudkar, Use of baculovirus BacMam vectors for expression of ABC drug transporters in mammalian cells, *Drug Metab. Dispos.* 40 (2012) 304–312.
- [37] J.J. Gribar, M. Ramachandra, C.A. Hrycyna, S. Dey, S.V. Ambudkar, Functional characterization of glycosylation-deficient human P-glycoprotein using a vaccinia virus expression system, *J. Membr. Biol.* 173 (2000) 203–214.
- [38] W.R. Skach, M.C. Calayag, V.R. Lingappa, Evidence for an alternate model of human P-glycoprotein structure and biogenesis, *J. Biol. Chem.* 268 (1993) 6903–6908.
- [39] Y. Xie, M. Burcu, D.E. Linn, Y. Qiu, M.R. Baer, Pim-1 kinase protects P-glycoprotein from degradation and enables its glycosylation and cell surface expression, *Mol. Pharmacol.* 78 (2010) 310–318.
- [40] J.D. Hirsch, L. Eslamizar, B.J. Filanoski, N. Malekzadeh, R.P. Haugland, J.M. Beechem, R.P. Haugland, Easily reversible desthiobiotin binding to streptavidin, avidin, and other biotin-binding proteins: uses for protein labeling, detection, and isolation, *Anal. Biochem.* 308 (2002) 343–357.
- [41] M. Fernandez-Suarez, T.S. Chen, A.Y. Ting, Protein–protein interaction detection in vitro and in cells by proximity biotinylation, *J. Am. Chem. Soc.* 130 (2008) 9251–9253.
- [42] E.J. Bowman, A. Siebers, K. Altendorf, Bafilomycins: a class of inhibitors of membrane ATPases from microorganisms, animal cells, and plant cells, *Proc. Natl. Acad. Sci. U. S. A.* 85 (1988) 7972–7976.
- [43] H. Hanada, Y. Moriyama, M. Maeda, M. Futai, Kinetic studies of chromaffin granule H⁺–ATPase and effects of bafilomycin A1, *Biochem. Biophys. Res. Commun.* 170 (1990) 873–878.
- [44] D.H. Lee, A.L. Goldberg, Proteasome inhibitors: valuable new tools for cell biologists, *Trends Cell Biol.* 8 (1998) 397–403.
- [45] P.D. Hart, M.R. Young, Ammonium chloride, an inhibitor of phagosome–lysosome fusion in macrophages, concurrently induces phagosome–endosome fusion, and opens a novel pathway: studies of a pathogenic mycobacterium and a nonpathogenic yeast, *J. Exp. Med.* 174 (1991) 881–889.
- [46] H. Peng, J. Qi, Z. Dong, J.T. Zhang, Dynamic vs static ABCG2 inhibitors to sensitize drug resistant cancer cells, *PLoS One* 5 (2010) e15276.